

G^2 Interpolation for polar surfaces

Jianzhong Wang¹  and Fuhua Cheng^{1,2} 

¹University of Kentucky; ²National Tsinghua University

ABSTRACT

In this paper, we present a G^2 interpolating scheme for Polar surfaces, so that polar surfaces can be used in high precision CAD/CAM applications as well. The new scheme is Bezier crust based, i.e., the interpolating surface is generated by parametrically attaching an especially selected bi-degree 5 Bezier surface to a Catmull-Clark subdivision surface. While Bezier crust based scheme handles quad faces only, we show that through a conversion process, we can handle triangular faces in the Polar part as well. Curvature continuity of the generated limit surface of our new scheme is consistent with the corresponding Polar surface. In case of a PCCS, the generated limit surface of our new scheme is G^2 on the Polar part.

KEYWORDS

Subdivision; Polar surface; interpolation; PCCS

1. Introduction

Subdivision surfaces have been widely used in CAD, gaming and computer graphics. Catmull-Clark subdivision (CCS) [2], based on tensor product bi-cubic B-Splines, is one of the most widely used subdivision schemes. The surfaces generated by the scheme are C^2 continuous everywhere except at extraordinary points, where they are C^1 continuous. A shortcoming inherent in CCS surfaces is the ripple problem, that is, ripples tend to appear around an extraordinary point with high valence. In the past, research focused on improving curvature distribution at extraordinary points. However, with quad mesh structure of CCS surfaces, ripples could not be avoided in high valence cases. To handle this artifact, Polar surface are studied by a number of researchers.

A Polar surface has a quad/triangular mixed mesh structure. A bi-cubic Polar subdivision scheme is presented in [6] which sets up the control mesh refinement rules for Polar configuration so that the limit surface is C^1 continuous and curvature bounded. A Polar surface handles high valence cases well, but there are some issues to solve for connecting them to Catmull-Clark meshes. For instance, because of the mismatch on the mesh between radial subdivision and Catmull-Clark subdivision, in [7], given a polar vertex of valence n , at the k^{th} level, its generalized bi-cubic subdivision scheme generates 2^k subfaces and expands the valence to $2^k n$. Recently a new subdivision scheme was developed in [11]. This new scheme, named PCCSS, subdivides triangular faces

in Polar embedded Catmull-Clark (PCC) mesh without generating exponential number of subfaces and without doubling valences in each subdivision step, and its limit surface is G^2 at Polar extraordinary points.

The polar surface can handle high valence very well. However, all current polar subdivision schemes are approximating, i.e. the generated limit surface will not interpolate the given control mesh. Given the complexity of quad/triangular mesh structure, no known interpolation scheme was developed yet. But, since many applications require an interpolation scheme, Polar surface is not well adopted in CAD/CAM. In this paper, we present a G^2 interpolating scheme on Polar surface, such that it can be used in high precision CAD/CAM application. Our new scheme is based on Bezier crust [12][13], where an interpolating surface was generated by parametrically adding Catmull-Clark subdivision surface and a special selected bi-degree 5 Bezier surface. Although scheme of Bezier crust handles quad faces only, we show by conversion, we can handle triangular faces in Polar mesh as well. The curvature continuity of generated limit surface of our new scheme is consistent with the corresponding Polar surface, in case of the PCCS [11], it is G^2 on Polar extraordinary points, C^1 at CCS extraordinary points, and everywhere else C^2 .

The rest of the paper is organized as follows. Section 2 reviews Polar surface and Bezier crust, Section 3 introduces our new G^2 interpolating scheme on Polar surface, especially on PCCS, Section 4 evaluates the behavior of the new interpolation surface, Section 5 concludes.

2. Polar surface and PCCSS

In this section, we review earlier works on Polar surfaces.

A Polar surface has the following properties on its mesh structure: faces adjacent to extraordinary points are triangular, all other faces are regular. A typical Polar mesh is shown in Fig. 2(a). A Polar surface has a quad/triangular mixed mesh structure. [8] introduces the concept of Polar surface. A bi-cubic Polar scheme is presented in [6] that sets up the control mesh refinement rules for Polar configuration such that the limit surface is C^1 continuous and curvature bounded. A C^2 Polar surface is shown in [9] by modifying weights of the Polar subdivision for different valences.

Traditional Polar surface can handle high valence ripple problems inherent in Catmull-Clark Subdivision (CCS) surfaces very well, but it is difficult to design a traditional Polar surface for a complex object with thousand of control points. Efforts are made to combine Polar meshes and CCS meshes. In [7], mesh refinement on Polar part is done in two steps at the k^{th} level, (1) k times radially, then (2) k times circularly. This scheme doubles

valence in each subdivision steps, i.e. given a Polar vertex of valence n , after k subdivisions, the Polar valence is expanded to $2^k n$. Recently a new scheme is presented in [11], this new scheme works on Polar/CCS hybrid mesh structure (as shown in Fig. 2(c)), named as Polar Embedded Catmull-Clark Subdivision (PCC) mesh. PCC mesh allows extraordinary points to exist also in the quad mesh part. The new subdivision scheme PCCS [11] comes with the following properties and improvements: (1). In each subdivision step, the Polar valence does not double, instead, it remains the same. (2). Only $O(k)$ sub-surfaces are generated after k subdivisions. (3). A natural C^2 join between Polar part and CCS part.

The subdivision scheme of PCCSS works as follows. Given an arbitrary mesh, first step is to convert it to CCS mesh with all quad faces and no two extraordinary points neighboring to each other, this is done by up to twice CCS subdivisions. Then, we replace faces surrounding high valence extraordinary points with Polar structure shown in Fig. 2(a). The obtained PCC mesh structure is shown in Fig. 2(c).

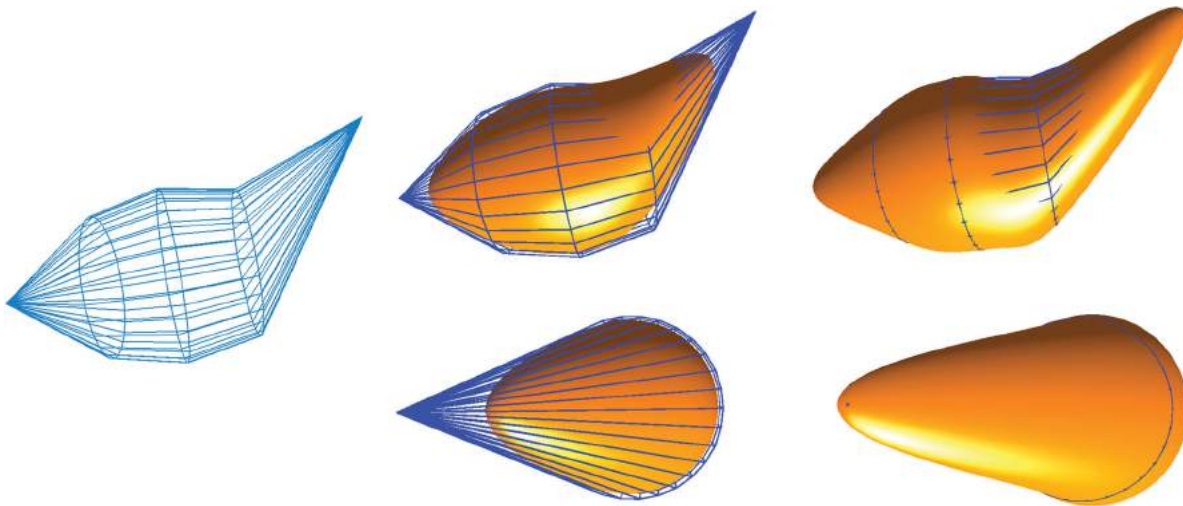


Figure 1. A Polar example. Left: Polar mesh; middle: two views of PCCS surface; right: two views of our new Interpolation surface.

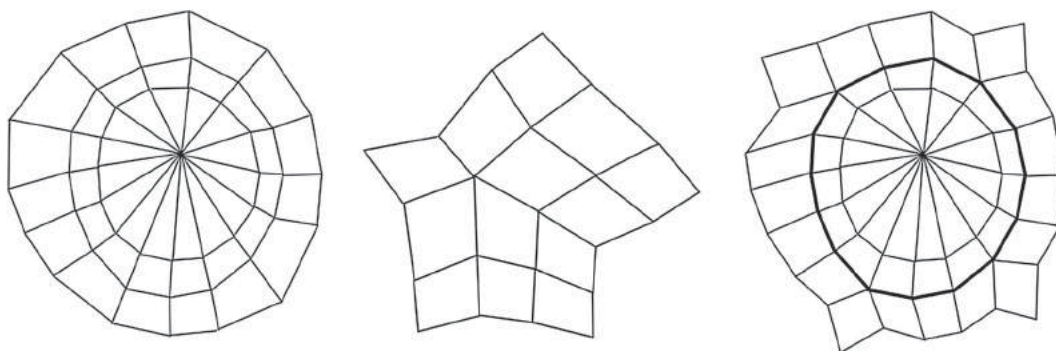


Figure 2. From left to right: Polar mesh, CCS mesh, PCC mesh.

PCC mesh is more generalized than both CCS mesh and Polar mesh. If PCC mesh has Polar extraordinary points, then it is Polar mesh, and if PCC mesh has only CCS extraordinary points, then it is CCS mesh. So in this paper, we focus our work on the subdivision surface PCCSS on PCC mesh.

The Polar extraordinary point can have a valence of even or odd. Since the odd valence is more difficult to achieve in terms of curvature continuity, a preprocessing step is performed by a special subdivision (Fig. 3). The new edge points, face points and vertex points of a Polar face with valence n are defined by CCS rules on arbitrary topology, e.g. new face point $P_{33}' = \frac{1}{3}(V + P_{32} + P_{33})$, new edge point $P_{32}' = \frac{1}{4}(V + P_{32} + P_{31}' + P_{33}')$, and new vertex point $V' = \frac{n-2}{n}V + \frac{1}{n}\bar{E} + \frac{1}{n}\bar{F}'$ (where \bar{E} is the average of original edges points, and \bar{F}' is the average of new face points). In contrast with CCS, we divide the Polar face into 4 sub-faces (the right of Fig. 3) which maintains the Polar structure and doubles the valence of Polar extraordinary point. With this special subdivision, the new faces points generated will be treated as edge points of new Polar triangular faces.

After valence conversion, the PCCSS uses Guided U-subdivision (GUS) for consequent subdivisions. The GUS is shown in Fig. 4. Each GUS will generate 5 layers of control points, control points in the last three layers (red dots in Fig. 4(a)) are generated by CCS equivalent U-subdivision on the first three layers of last subdivision step (black circles in Fig. 4(a)). The control points

in the first layer (blue dots in Fig. 4(a)) are selected from the dominative control meshes (as shown in Fig. 4(b)). The control points in the second layers of are selected by a process called *virtual U-Subdivision*, i.e. these control points are reverse calculated from the new 1st layer control points and the last three layer control points in previous GUS.

In [11], it shows that the limit surface of PCCSS as above is C^2 everywhere except at extraordinary points, where it is G^2 at Polar extraordinary points and C^1 at CCS extraordinary points.

3. A Heuristic interpolation scheme on pccss

Subdivision schemes can be classified into two types. If the original vertices in the control mesh is the same as its corresponding limit points after subdivisions, we call such scheme interpolating, otherwise, the scheme is approximating. Current Polar schemes are all approximating. Although Polar surface can handle high valence ripples common in Catmull-Clark Subdivision surface, for high precision CAD/CAM usage, an interpolating scheme is highly desirable. Due to the triangle/quad mixed mesh structure, no known interpolating scheme was developed so far. In this section, we present a heuristic G^2 interpolation scheme on PCCSS.

In PCCSS, A PCC mesh can be separated into two parts, Polar part and CCS part. The limit surface on CCS part is exactly the same as that of the CCSS. So it makes it possible to construct an interpolating scheme at quad faces the same as the interpolating scheme for CCSS. Interpolation of CCSS is traditionally performed by solving a global linear system of

$$Ax = b \tag{3.1}$$

Where A is the coefficient matrix determined by CCS subdivision rules, x is the column vector of control points to be determined, and b is the column vector of data points in the given data mesh [5]. Stationary iterative methods like Jacobi, Gauss-Seidel or Successive Over-relaxation can be used to solve equation (3.1).

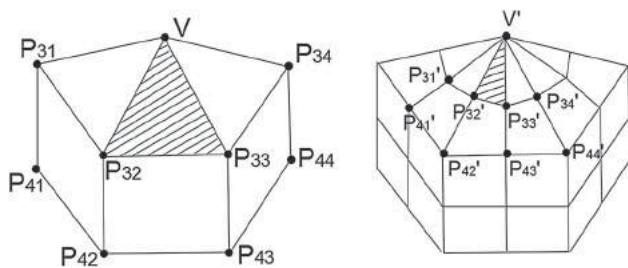


Figure 3. Convert odd Polar valence to even by one subdivision.

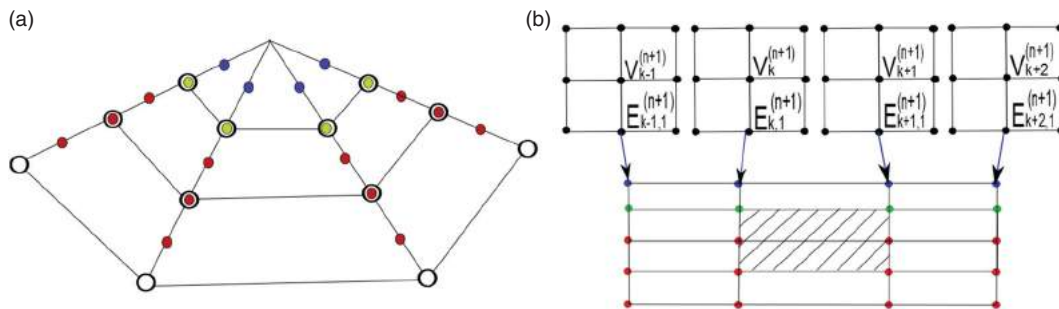


Figure 4. From left to right: (a) Guided U-Subdivision (b) select 1st layer control points in GUS.

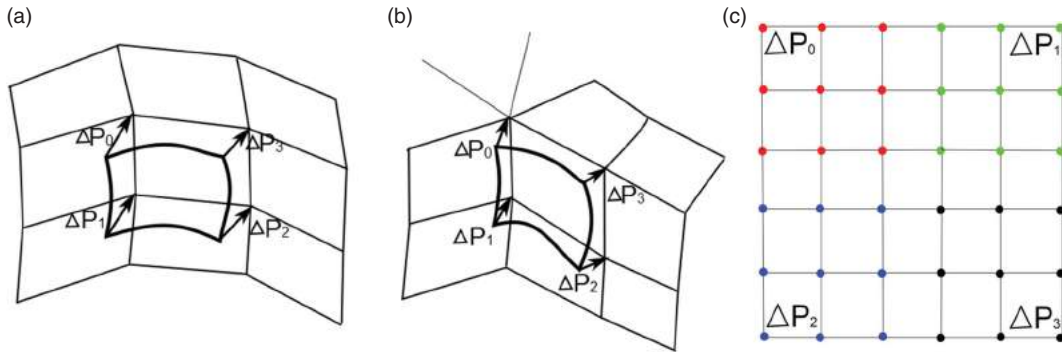


Figure 5. Difference Vectors between control points and limit points, from left to right: (a) regular face (b) extraordinary face (c) offsetting Bezier Crust.

However when data set is large, the convergence rate of above methods is slow. Some faster iterative methods [1][3][4][10] were developed to improve the convergence rate. However, the iterative methods above suffer excessive undulation [5]. To improve the shape of interpolation surface, fairing techniques are required and the final shape of interpolation surface are non-predictable. Recently, a direct interpolation scheme called Bezier Crust is introduced in [12]. The idea of new scheme is to apply a bi-degree 5 piecewise specially selected Bezier Surface on CCSS, such that the interpolation surface can be generated in one step instead of iterations.

Piecewise bi-degree 5 Bezier surface is the necessary condition to obtain a G^2 limit surface, but its computation is generally costly and not a simple task. Bezier crust is a simplified Bi-degree 5 Bezier surface, in that its 1st and 2nd order derivatives vanishes at boundaries of each patch. Given a CCS mesh M , The limit surface of each face f of M (regular or extraordinary) can be represented in parametric form $S(u, v)$. For each f , $\Delta P_0, \Delta P_1, \Delta P_2$ and ΔP_3 are defined as the difference vectors between the corner control points and their corresponding CCS data points, respectively. In order to interpolate the control points, a bi-quintic Bezier crust $\Delta S(u, v)$ is defined as follows,

$$\Delta S(u, v) = \sum_{i=0}^5 \sum_{j=0}^5 b_{i,5}(u)b_{j,5}(v)\Delta P_{i,j} \quad (3.2)$$

With $\Delta P_{i,j}$ takes value of $\Delta P_0, \Delta P_1, \Delta P_2$ and ΔP_3 . $\Delta P_{i,j} = \Delta P_0$ if $i \in [0, 2]$ & $j \in [0, 2]$; $\Delta P_{i,j} = \Delta P_1$ if $i \in [0, 2]$ & $j \in [3, 5]$; $\Delta P_{i,j} = \Delta P_2$ if $i \in [3, 5]$ & $j \in [0, 2]$; $\Delta P_{i,j} = \Delta P_3$ if $i \in [3, 5]$ & $j \in [3, 5]$. $\Delta P_0, \Delta P_1, \Delta P_2$ and ΔP_3 are the difference vectors at four corners of a CCS face (Fig. 5).

With offsetting Bezier crust $\Delta S(u, v)$ defined, the interpolating parametric surface $\bar{S}(u, v)$ can be expressed

as follows:

$$\bar{S}(u, v) = S(u, v) + \Delta S(u, v) \quad (3.3)$$

The offsetting Bezier Crust has the following properties:

- 1) 1st order and 2nd order derivatives vanish across the face boundaries and at 4 corners.
- 2) Underlying subdivision rules independent, can handle arbitrary quad subdivision surfaces.
- 3) C^2 on each Bezier Crust limit face.

The new CCS interpolation surface obtained by equation (3.3) has the following properties:

- 1) C^2 everywhere except at extraordinary points, where it is C^1 continuous
- 2) Interpolates not only data points, but also the surface normal and curvature at these data points.

Since PCCSS has the same limit surface as CCS at quad face part, so on quad faces, equation (3.3) can be applied to obtain its interpolation limit surface. For Polar faces, these faces are triangular, equation (3.3) cannot be applied directly. However, we note that the PCCSS treats Polar faces as quad faces by technique of vertex splitting (Fig. 6).

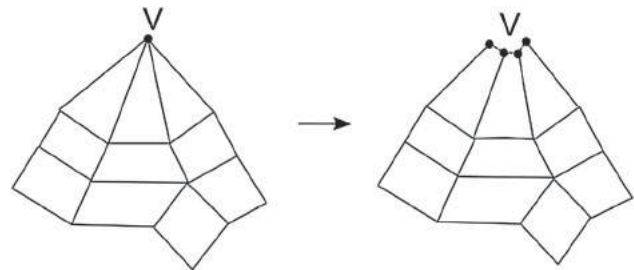


Figure 6. Polar face conversion by vertex splitting.

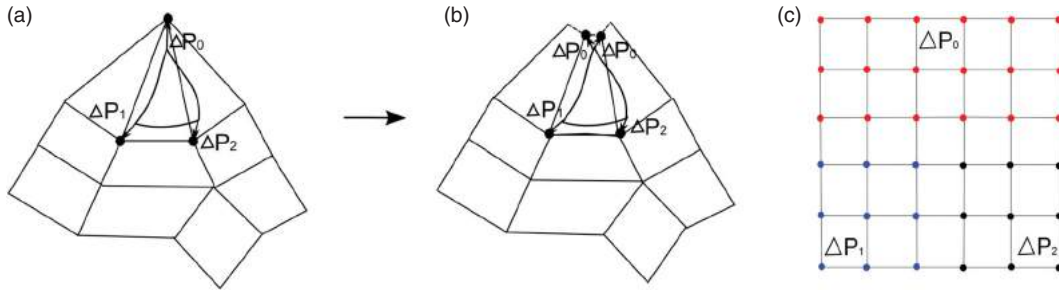


Figure 7. From left to right: (a) difference vectors on Polar face, (b) vertex splitting of difference vectors in (a), (c) bi-quintic offsetting Bezier Crust on Polar face.

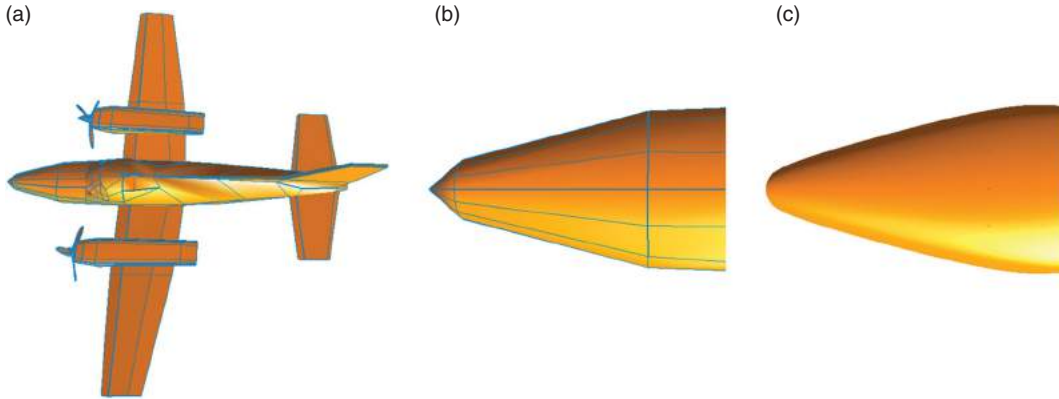


Figure 8. From left to right: (a) A PCC mesh of an airplane (b) enlarged plane head with Polar configuration, (c) interpolating limit surface with our new scheme on (b).

By vertex splitting in PCCSS, a Polar extraordinary point V is duplicated at each Polar face, such that the Polar face can apply Bezier Crust as well. The limit surface of each Polar face f in PCCSS can be represented in parametric form $S(u, v)|_{polar}$. For each f , ΔP_0 , ΔP_1 , and ΔP_2 (Fig. 7(a)) are defined as the difference vectors between the corner control points and their corresponding PCCSS limit points respectively. By vertex splitting of ΔP_0 (Fig. 7(b)), we obtain 4 difference vectors on each converted quad face (Fig. 7(c)). In order to interpolate the difference vectors at corners of Polar face f , a bi-quintic Bezier crust $\Delta S(u, v)|_{polar}$ is defined as follows,

$$\Delta S(u, v)|_{polar} = \sum_{i=0}^5 \sum_{j=0}^5 b_{i,5}(u) b_{j,5}(v) \Delta P_{i,j} \quad (3.4)$$

With $\Delta P_{i,j}$ takes value of ΔP_0 , ΔP_1 , and ΔP_2 . $\Delta P_{i,j} = \Delta P_0$ if $i \in [0, 2]$; $\Delta P_{i,j} = \Delta P_1$ if $i \in [3, 5]$ & $j \in [0, 2]$; $\Delta P_{i,j} = \Delta P_2$ if $i \in [3, 5]$ & $j \in [3, 5]$. ΔP_0 , ΔP_1 , ΔP_2 are the difference vectors at four corners of a converted Polar face (Fig. 7).

With offsetting Bezier crust on a Polar face $\Delta S(u, v)|_{polar}$ defined, the interpolating parametric surface on a Polar face $\bar{S}(u, v)|_{polar}$ can be expressed as

follows:

$$\bar{S}(u, v)|_{polar} = S(u, v)|_{polar} + \Delta S(u, v)|_{polar} \quad (3.5)$$

Given a PCC mesh, with equation (3.4) defining Bezier Crust on Polar face and equation (3.2) defining Bezier Crust on Quad face, one can construct a piecewise offsetting bi-quintic Bezier Crust on PCCSS to interpolate difference vectors between PCC mesh control points and their PCCSS limit points. By parametrically adding Bezier Crust to PCCS limit surface (equation (3.3) and (3.5)), one can obtain an interpolating limit surface with properties as follows,

- 1) C^2 continuous everywhere, except at extraordinary points, where it is G^2 on Polar extraordinary points, C^1 at CCS extraordinary points.
- 2) It interpolates control points in PCC mesh, and interpolates the normals and curvature at their corresponding data points at PCCS limit surface.

Above we introduce our new interpolation scheme for PCCSS. Fig. 8 shows an airplane with Polar part on plane head, the new interpolating surface of plane head (Fig. 8(c)) is smooth and without ripples. Since most Polar subdivision scheme uses vertex splitting to match

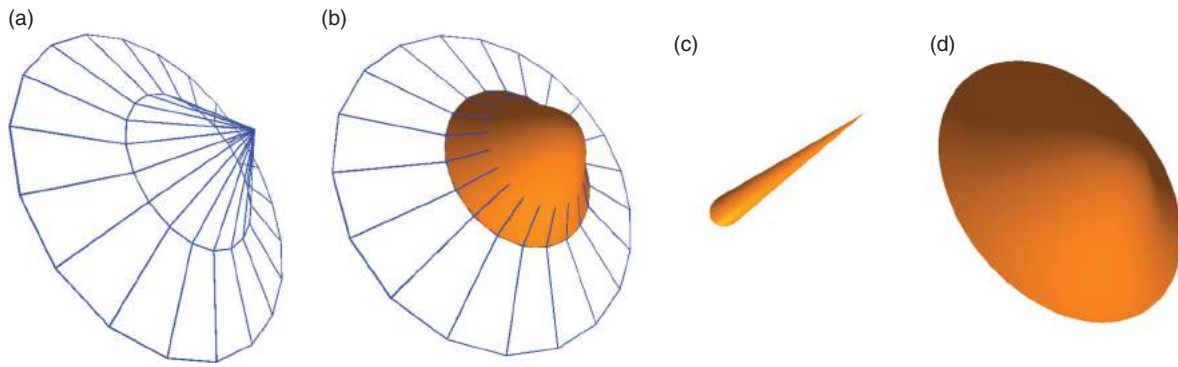


Figure 9. From left to right: (a) Polar mesh (b) new interpolating surface (c) Bezier Crust shown alone (enlarged) (d) Bezier Crust is shown on projected flat PCCSS limit surface (enlarged).

quad and triangular faces and Bezier Crust is subdivision rules independent, the above methods can be applied to these scheme.

4. Implementation and analysis

In previous section, we introduced the concept of our new interpolation surface for PCCSS. This new interpolation surface is generated by parametrically adding a piecewise offsetting Bezier Crust to PCCS limit surface. Given a PCC mesh M , for each (u, v) of quad face or converted Polar face (vertex splitting), the interpolating algorithm is implemented as follows:

- 1) Compute $S(u, v)$ limit point for each (u, v)
- 2) Compute difference vectors on all control points in M
- 3) Derive Bezier Crust on converted difference vectors
- 4) Computer $\Delta S(u, v)$ on derived Bezier Crust
- 5) Obtain $\bar{S}(u, v)$ by adding $S(u, v)$ and $\Delta S(u, v)$

With the special selection of Bezier Crust, the computation of each limit point on interpolation surface only increase constant time $O(1)$ to the computation of each PCCSS limit point. So the running cost of adding a Bezier Crust in our new scheme is not expensive.

Fig. 9(a) shows a typical Polar mesh. Fig. 9(b) shows the interpolating surface generated by our new interpolation scheme. Fig. 9(c) shows the limit surface of Bezier Crust when it is shown standalone. We see that when Bezier Crust is drawn standalone, the limit surface is actually only G^0 continuous. This is consistent with the duplications of control points at 4 corners. However, when we show the Bezier crust (Fig. 9(c)) parametrically added to the PCCSS limit surface of a flat mesh converted by projection of this Polar mesh onto (x, y) plane. We see that although the underlying PCCS limit surface of projected flat mesh has zero Gaussian curvature everywhere

and Bezier crust is only G^0 continuous, the parametrically added interpolating surface is smooth (Fig. 9(d)).

As stated in the last section, the new interpolating surface on PCC mesh has two properties. Here we provide a proof. Given a Polar face f_i after vertex splitting (as shown in Fig. 10), We define $D_{(i,j)}(x, y)|S$ as partial derivative of i^{th} and j^{th} order with respect to u and v respectively at parametric value (x, y) on PCCS surface $S(u, v)$, $u, v \in [0, 1]$. Similarly we can define $D_{(i,j)}(x, y)|\Delta S$ and $D_{(i,j)}(x, y)|\bar{S}$ as the partial derivative at (x, y) on Bezier Crust $\Delta S(u, v)$ and our new interpolating surface $\bar{S}(u, v)$.

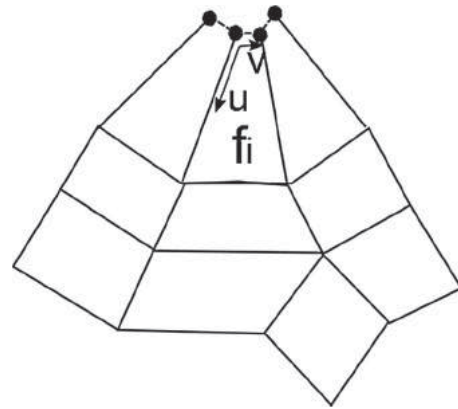


Figure 10. Parametric Polar face after vertex splitting.

Property 1: Our new interpolating surface is C^2 continuous everywhere, except at extraordinary points, where it is G^2 on Polar extraordinary points, C^1 at CCS extraordinary points.

Proof: Since PCCS separate surface into two parts: CCS part and Polar part [11]. For CCS part, as proven in [12], interpolating surface maintains the continuity of its underlying CCS surface, which is C^2 continuous everywhere, except at CCS extraordinary points, where it is C^1 only. Next we show the surface continuity on Polar face part.

For Polar part of PCCSS, it is C^2 continuous everywhere and C^2 continuous with its neighboring CCSS patches, except at Polar extraordinary points. So, as proven in [12], its interpolating surface by appending Bezier Crust is also C^2 continuous everywhere, except at Polar extraordinary points.

As illustrated in Fig. 10, a Polar face f_i is converted to quad face with vertex splitting and can be (u, v) parameterized. The Polar extraordinary point on PCCSS can be represented by $S(0, v)$, $v \in [0, 1]$. With equation (3.4), the 1st order and 2nd order partial derivatives of Polar Bezier Crust $\Delta S(u, v)$ has the following values at $(0, v)$,

$$D_{(1,0)}(0, v)|\Delta S = 0, D_{(0,1)}(0, v)|\Delta S = 0, D_{(2,0)}(0, v) \times |\Delta S = 0, D_{(1,1)}(0, v)|\Delta S = 0, D_{(0,2)}(0, v)|\Delta S = 0.$$

With equation (3.5), our new interpolating surface at Polar extraordinary point $\tilde{S}(0, v)$ computed has the same 1st order and 2nd order derivatives as its underlying PCCSS at Polar extraordinary point $S(0, v)$. Since PCCSS is G^2 continuous at Polar extraordinary points, we can conclude that our new interpolating surface is also G^2 continuous at Polar extraordinary points. QED

Property 2: It interpolates control points in PCC mesh, and interpolates the normal and curvature of their corresponding limit points at PCCS limit surface.

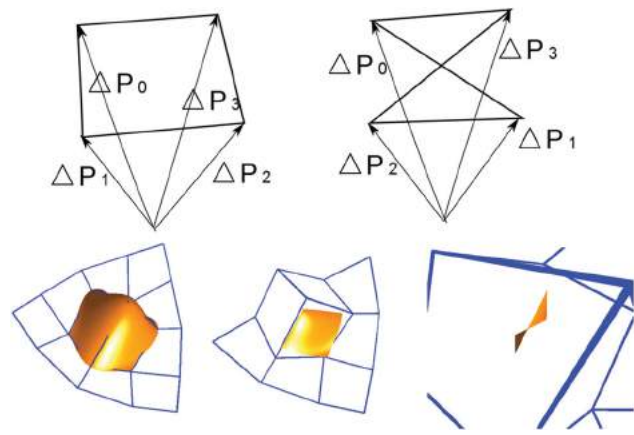


Figure 11. Top shows two scenario of difference vectors; bottom shows an interpolating example, left is our new interpolating surface, middle is the CCS limit surface, right is Bezier Crust shown standalone.

Proof: Since the 1st order and 2nd order derivatives of Bezier Crust vanishes at 4 corners, by analyzing equation (3.5), we can conclude that 1st order and 2nd order derivatives of PCCS limit surface on the corner control points of each face are the same as those of our new interpolating surface. QED

Since PCC mesh is an extension to Polar mesh by including CCS extraordinary points. So we can apply our new interpolating scheme on Polar mesh as well.

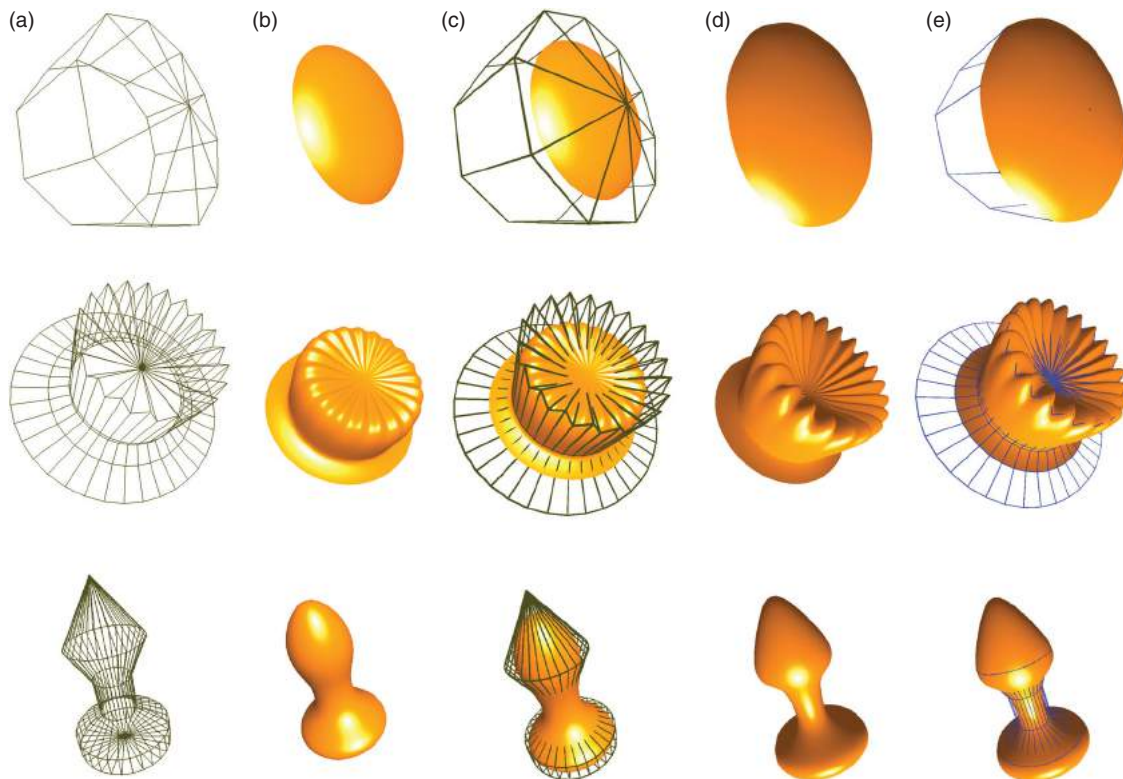


Figure 12. Three examples of interpolating on Polar mesh, (a) Polar mesh, (b) Polar limit surface with PCCSS, (c) mesh with limit surface together, approximating, (d) new interpolating limit surface with Bezier Crust on PCCSS (e) mesh shown with interpolating surface.

Corollary 1: On Polar mesh, our new interpolating surface is C^2 continuous everywhere, except at Polar extraordinary points, where it is G^2 .

Proof: A Polar mesh is a PCC mesh without CCS extraordinary points. PCCS can be applied to Polar mesh as well. On a Polar mesh, the PCCSS is C^2 continuous everywhere, except at Polar extraordinary points, where it is G^2 . With **Property 1** shown above, one can prove that our new interpolating surface on Polar mesh is C^2 continuous everywhere, except at Polar extraordinary points, where it is G^2 . QED

Implementation results (Fig. 1, 8, 9, 12) show that our new interpolating scheme can generate high quality Polar limit surface. Our new interpolating scheme on PCC mesh is heuristic, it can efficiently compute each limit point of interpolating surface without drastically adding computation time.

The shape of Bezier Crust shown standalone depends on difference vectors. Twisting effect may happen on Bezier Crust when difference vectors take opposite directions (bottom right of Fig. 11)[12]. But this twisting effect can be compensated by underlying subdivision surfaces. So generally, such twisting effect is not visible in the generated interpolating surfaces. More experiments and further research are needed for identifying the impact of twisting effects on our new interpolating surfaces.

5. Conclusion

In this paper, we introduce a new heuristic interpolation scheme on Polar surfaces, especially on PCCSSs. We show that, by vertex splitting, we can treat a Polar face as a quad face, such that the bi-quintic offsetting Bezier Crust can be applied to the Polar faces as well. The generated interpolating surface maintains the continuity of underlying PCCS limit surface, i.e. G^2 on Polar extraordinary points, C^1 on CCS extraordinary points, and C^2 everywhere else.

Implementation results show that our new scheme can generate high quality images appropriate for engineering and computer graphics usage.

While Polar surface is studied to solve high valence artifact inherent in CCS, no known work is developed for interpolation schemes on Polar surfaces. With our subdivision independent interpolation scheme of Bezier Crust, we can efficiently generate a smooth interpolating surface on a PCC/Polar mesh.

Acknowledgment

This work is supported by National Science Foundation of China (61020106001, 61170324), National Science Council

of ROC (NSC-100-2811-E-007-021), and a joint grant of National Tsinghua University and Chang-Gung Memorial Hospital (101N2756E1).

ORCID

Jianzhong Wang  <http://orcid.org/0000-0002-4250-7956>

Fuhua Cheng  <http://orcid.org/0000-0003-2098-3027>

References

- [1] Beck, A.; Teboulle, M.: A fast iterative shrinkage-thresholding algorithm for linear inverse problems, *SIAM Journal on Image Sciences*, 2(1), 2009, 183–202. <http://dx.doi.org/10.1137/080716542>
- [2] Catmull, E.; Clark, J.: Recursively generated B-spline surfaces on arbitrary topological meshes, *Computer-Aided Design*, 10(6), 1978, 350–355. [http://dx.doi.org/10.1016/0010-4485\(78\)90110-0](http://dx.doi.org/10.1016/0010-4485(78)90110-0)
- [3] Chen, Z.; Luo, X.; Tan, L.; Ye, B.; Chen, J.: Progressive interpolation based on Catmull-Clark subdivision surfaces, *Computer Graphics Forum*, 27, 2008, 1823–1827.
- [4] Cheng, F.; Fan, F.; Lai, S.; Huang, C.; Wang, J.; Yong J.: Loop subdivision surface based progressive interpolation, *Journal of Computer Science and Technology*, 24(1), 2009, 39–46. <http://dx.doi.org/10.1007/s11390-009-9199-2>
- [5] Halstead, M.; Kass, M.; Deroose, T.: Efficient, fair interpolation using Catmull-Clark surfaces, In proceedings of the 20th annual conference on Computer graphics and interactive techniques, ACM, p. 44.2, 1993.
- [6] Karciauskas, K.; Peters, J.: Bicubic polar subdivision, *ACM Transactions on Graphics*, 26(4), 2007, 14. <http://dx.doi.org/10.1145/1289603.1289605>
- [7] Myles, A.; Karciauskas, K.; Peters, J.: Pairs of bi-cubic surface constructions supporting polar connectivity, *Computer Aided Geometric Design*, 25(8), 2008, 621–630. <http://dx.doi.org/10.1016/j.cagd.2008.06.002>
- [8] Peters, J.; Karciauskas, K.: An introduction to guided and polar surfacing, *Mathematics Methods for Curves and Surfaces*, 299–315, 2010.
- [9] Peters, J.; Myles, A.: Bi-3 C^2 Polar subdivision, *ACM Trans. Graph*, 28(3), 2009, 1–12.
- [10] Szeliski, R.: Fast surface interpolation using hierarchical basis functions, *IEEE Transactions on Pattern Analysis and Machine Intelligence*, 12(6), 1990, 513–528.
- [11] Wang, J.; Cheng, F.: Polar Embedded Catmull-Clark Subdivision Surface, *Computer-Aided Design and Computer Graphics (CAD/Graphics)*, 2013 International Conference on. *IEEE*, 2013. <http://dx.doi.org/10.1109/CADGraphics.2013.99>
- [12] Wang, J.; Cheng, F.: Bezier Crust on Quad Subdivision Surface, *Pacific Graphics Short Papers. The Eurographics Association*, 2013. <http://dx.doi.org/10.2312/PE.PG.PG2013short.029-034>
- [13] Wang, J.; Cheng, F.: A Heuristic Offsetting Scheme for Catmull-Clark Subdivision Surfaces, *Computer-Aided Design & Applications*, 12(6), 2015, 765–771. <http://dx.doi.org/10.1080/16864360.2015.1033342>